

## FIRST PHOTOMETRIC INVESTIGATION OF TWO ECLIPSING BINARY SYSTEMS CRTS J213033.6+213159 AND 1SWASP J212454.61+203030.8

Massimiliano Martignoni<sup>1</sup>, Carlo Barani<sup>1</sup>, Francesco Acerbi<sup>1</sup>, and Raúl Michel<sup>2</sup>

*Received May 1 2020; accepted June 1 2020*

### ABSTRACT

The multicolour CCD light curves of the eclipsing binary systems CRTS J213033.6+213159 and 1SWASP J212454.61+203030.8 are presented for the first time, the observations are analyzed using the latest version of the Wilson-Devinney code. Both the systems are found to be W UMa contact binaries belonging to two different subtypes. All the light curves show the inverse O’Connell effect. By using our 2 times of minimum light for both the systems and the 187 and 105 ToMs extract from the SWASP observations, respectively for CRTS J213033.6+213159 and for 1SWASP J212454.61+203030.8, the orbital periods are here revised. The spectral type K of the systems and their short orbital periods ( $<0.3$  days), suggests that they are near the shortest period limit. The absolute dimensions are estimated and, from statistical diagrams, it is found that both components of the systems follow the general pattern of the relative subtype of W Ursae Majoris systems.

### RESUMEN

Se presentan las primeras curvas de luz multicolor de las binarias eclipsantes CRTS J213033.6+213159 y 1SWASP J212454.61+203030.8, analizadas con la última versión del código Wilson-Devinney. Se encuentra que ambos sistemas son binarias en contacto tipo W UMa pero de diferente subtipo. Todas las curvas de luz presentan el efecto O’Connell inverso. Con nuestros dos tiempos de mínima luz junto con los 187 y 105 tiempos, extraídos de las observaciones SWASP, de CRTS J213033.6+213159 y 1SWASP J212454.61+203030.8 respectivamente, se hace una revisión de los periodos orbitales. El tipo espectral de los sistemas (K) y sus cortos periodos orbitales ( $< 0.3$  días), sugieren que se encuentran cerca del límite inferior del periodo. También se estiman sus dimensiones absolutas y, a partir de diagramas estadísticos, se encuentra que ambas componentes de estos sistemas siguen el patrón general de los objetos W Ursae Majoris.

*Key Words:* techniques: photometric — binaries: eclipsing — stars: individual: CRTS J213033.6+213159, 1SWASP J212454.61+203030.8

### 1. INTRODUCTION

Contact binaries can be classified into four categories: A-subtype and W-subtype proposed by Binnendijk (1965) in which, in general, the A-subtype shows a transit at primary minimum with mass ratio  $q < 0.3$  and periods  $> 0.3$  days, the opposite is true for W-subtype. B-subtype proposed by Lucy & Wilson (1979) are systems in geometrical but not in thermal contact, with large surface temperature differences

between the components. H-subtype, proposed by Csizmadia & Klagyvik (2004), are systems in which the predominant characteristic is a large mass ratio  $q > 0.72$ .

Speaking generally, among the A-subtype, is possible to find the deep low-mass-ratio (DLMR) contact binaries, which are systems with a high fill out factor ( $f > 50\%$ ) and a low mass ratio ( $q < 0.25$ ) as proposed by Qian et al. (2005) and may be the progenitors of single rapidly rotating stars (Stępień 2011, Tyłenda et al. 2011, Zhu et al. 2016, Liao et al. 2017).

<sup>1</sup>Stazione Astronomica Betelgeuse, Magnago, Italy.

<sup>2</sup>Instituto de Astronomía, Universidad Nacional Autónoma de México, México.

TABLE 1  
 $UBV(RI)_C$  AND 2MASS MAGNITUDES OF THE FIELD STARS

ID	Name	RA (2000)	DEC (2000)	$U$	$B$	$V$	$R_c$	$I_c$	$J$	$H$	$K_s$
1	J213033	322.640089	+21.533081	16.218	15.597	14.623	14.030	13.497	12.662	12.174	12.039
2	2MASSJ21304078+2132332	322.669929	+21.542580	16.690	15.962	14.946	14.364	13.825	12.981	12.447	12.318
1	J212454	321.227186	+20.508471	17.334	16.763	15.808	15.211	14.642	13.494	13.039	12.849
2	2MASSJ21245253+2031522	321.218961	+20.531240	15.153	14.519	13.561	12.971	12.471	11.682	11.127	11.059

The eclipsing binary star CRTS J213033.6+213159 (hereinafter J213033,  $\alpha_{2000} = 21^h30^m33^s.6$ ,  $\delta_{2000} = +21^\circ31'59''.2$ ) is listed as a variable star with a period of 0.2246940 days and an amplitude of variation of 0.27 mag. in the Catalina Surveys Periodic Variable Star Catalog (Drake et al. 2014)

1SWASP J212454.61+203030.8 (hereinafter J212454,  $\alpha_{2000} = 21^h24^m54^s.61$ ,  $\delta_{2000} = +20^\circ30'30''.8$ ) was proposed as a short period variable star in the list of candidate eclipsing binaries published by Norton et al. (2011), with a period and amplitude of variation of 0.22783 days and 0.15 mag.

A light curve for this system was reported by Lohr et al. (2013), which presented the typical EW-type behavior.

With no previous studies on these systems, the aim of the present work is to analyze their light curves using the latest version of the Wilson-Devinney code and to understand the geometrical structure and evolutionary state of these eclipsing binaries. The determination of parameters of contact systems, though resulting only from the light curve solutions, can be useful to improve the empirical relations of overcontact W UMa systems.

## 2. CCD PHOTOMETRIC OBSERVATIONS AND DATA REDUCTION

Observations were carried out at the San Pedro Martir Observatory with the 0.84-m telescope, a filter-wheel and the *Spectral Instruments 1* CCD detector (a deep depletion e2v CCD42-40 chip with gain of  $1.39 \text{ e}^-/\text{ADU}$  and readout noise of  $3.54 \text{ e}^-$ ). The field of view was  $7.6' \times 7.6'$  and a binning of  $2 \times 2$  was used during all the observations. J212454 was observed on August 1 2017 for a total of 5.7 hours while J213033 was observed on the following night for a total of 6.5 hours. In both cases, alternated exposures in filters  $B$ ,  $V$ ,  $R_c$  and  $I_c$ , with exposure times of 20, 10, 6 and 6 seconds, respectively, were taken. Flat field and bias frames were also taken during both nights.

TABLE 2  
TIMES OF MINIMA OF J213033

HJD	Epoch(1)	O-C(1)	Error	Source
2457968.7484	-0.5	0.0029	0.0013	This work
2457968.8748	0	0.0017	0.0010	This work

All images were processed using IRAF<sup>3</sup> routines. Images were bias subtracted and flat field corrected before the instrumental magnitudes were computed with the standard aperture photometry method. These fields were also calibrated in the  $UBV(RI)_C$  system and the results, along with the 2MASS magnitudes, are presented in Table 1. Based on this information, we decided to use objects #2 as comparison stars, since they have magnitudes and colors similar to their respective variables, making differential extinction corrections negligible. Any part of the data set can be provided upon request.

From our observations of J213033 it was immediately clear that the period of 0.224 days proposed by the Catalina Catalog (Drake et al. 2014) was erroneous.

Using our new 2 ToMs presented in Table 2 and the 187 ToMs extracted from the 1SWASP (Butters et al. 2010) observations (more than 20000 measures, available as supplementary data, all heliocentric and determined with the polynomial fit method), we were able to refine the ephemeris of the system as follows:

$$\text{Min.}I(HJD) = 2457968.8731(0.0177) + 0^d.2551899(0.0000011) \times E. \quad (1)$$

For J212454 we used our 2 ToMs presented in Table 3 and the 105 ToMs extracted from the 1SWASP (Butters et al. 2010) observations (about 9500 measures available as supplementary data), that permitted us to refine the ephemeris, as shown in equation (2).

<sup>3</sup>IRAF is distributed by the National Optical Observatories, operated by the Association of Universities for Research in Astronomy, Inc., under cooperative agreement with the National Science Foundation.

TABLE 3  
TIMES OF MINIMA OF J212454

HJD	Epoch(2)	O-C(2)	Error	Source
2457966.8237	-0.5	-0.0003	0.0009	This work
2457966.9383	0	0.0005	0.0010	This work

$$\begin{aligned} \text{MinI}(HJD) = & 2457966.9379(0.0039) \\ & + 0^d.2278293(0.0000006) \times E + \\ & - 9.079^{-11}(2.139^{-11}) \times E^2. \quad (2) \end{aligned}$$

The ToMs used, presented in Table 3, are heliocentric and were determined with the polynomial fit method.

We used the data of Table 3 to show the behaviour of the  $O - C$  values, as shown in Figure 1. A parabolic trend can be inferred from this figure.

The data set covers only 13.2 years with a gap of 9.7 years between the last of our ToMs and the previous 1SWASP points. Bearing in mind this gap, it is impossible to see any observable manifestation due to cyclic orbital period variations, which seem to be present in many contact binaries. However, we have calculated an orbital period decrease at a rate of  $dP/dt = -2.91 \times 10^{-7}$  days  $\text{yr}^{-1}$ .

Such a variation can be explained by either mass transfer from the more massive secondary to the primary star or by angular momentum loss (AML) due to a magnetic stellar wind.

If the parabolic variation is produced by conservative mass transfer, the transfer rate is  $dM_2/dt = 2.34 \times 10^{-7} M_\odot \text{yr}^{-1}$  (Kwee 1958).

Assuming that the secondary star transfers its present mass to the less massive primary component on a thermal time scale (Paczynski 1971),  $\tau_{th} = 2 \times 10^{-7} M_2^2 (L_2 R_2)^{-1} = 4.84 \times 10^7$  years, mass is transferred to the companion at a rate of  $M_2/\tau_{th} = 1.69 \times 10^{-8} M_\odot \text{yr}^{-1}$ .

This value  $M_2/\tau_{th} M_\odot \text{yr}^{-1}$  is small compared the observed period change of  $dM_2/dt$ ; hence, a conservative mass transfer hypothesis is not confirmed.

Another possible mechanism for the parabolic variation is AML caused by magnetic braking. Guinan & Bradstreet (1988) derived an approximate formula for the period decrease rate due to spin-orbit-coupled AML of binary systems as follows:

$$\begin{aligned} dP/dt \approx & -1.1 \times 10^{-8} q^{-1} (1+q)^2 (M_1 + M_2)^{-5/3} k^2 \\ & \times (M_1 R_2^4 + M_2 R_1^4) P^{-7/3}, \quad (3) \end{aligned}$$

where  $k$  is the gyration constant. With  $k^2 = 0.1$ , (see Webbink 1976), and with the absolute dimensions of

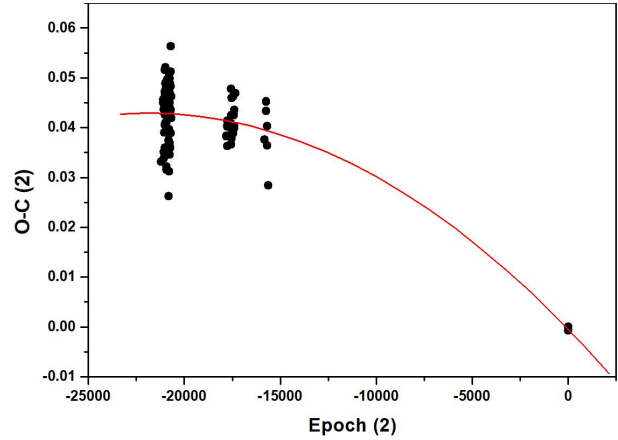


Fig. 1. The points are the data of Table 3. The solid line is the description by a second order polynomial fit to the new ephemeris in equation (2). The color figure can be viewed online.

Table 6 we computed the AML rate to be  $(dP/dt)$   $\text{AML} = -4.47 \times 10^{-8}$  days  $\text{yr}^{-1}$ , which is too small (compared with the observed value) by a factor of about 85%. Therefore, with AML alone it is difficult to fully explain the observed secular period decrease.

This means that neither mass transfer nor AML can describe the parabolic variation, indicating that the orbital period decrease could be as a combination of a downward parabola and a light-travel-time (LTT) effect due to a third body.

### 3. MODELLING THE LIGHT CURVES

Both the systems are newly discovered so there are no reported spectroscopic mass ratios for them; the latest version of the Wilson-Devinney Code (Wilson & Devinney 1971, Wilson 1990, Wilson & van Hamme 2015), was used for simultaneous modelling of our complete light curves.

The temperatures of the hotter components of both systems were estimated using the  $B - V$  index from APASS, the AAVSO Photometric All-Sky Survey (Henden et al. 2009), and interpolated from the tables of Worthey & Lee (2011).

We have taken into account the interstellar extinction using the period-color relation discovered by Eggen and revised by Wang (1994) as  $(B - V)_0 = 0.062 - 1.310 \log P$  (days). The results for both systems show that the interstellar extinction is negligible.

The atmospheric parameters adopted here were: from Lucy (1967) the gravity-darkening coefficients were taken to be 0.32 and the bolometric albedos were set to 0.5 (Ruciński 1973). The limb-darkening

TABLE 4  
DIFFERENCES IN THE HEIGHT OF THE  
MAXIMA (MAG.)

	J213033	J212454
MaxII - MaxI B	0.059	0.043
MaxII - MaxI V	0.046	0.033
MaxII - MaxI Rc	0.040	0.025
MaxII - MaxI Ic	0.038	0.016

parameters were interpolated with a square root law from the van Hamme (1993) tables for  $\log g = 4.0$  and solar abundances.

Inspection of the light curves indicates that they are similar in shape to the light curves of W UMa-type binary stars. This suggested to us to start the W-D analysis directly in Mode 3, suitable for over-contact binaries (W UMa stars).

The  $q$ -search method was applied to find the best initial value of  $q$  to be used during the light curve analysis.

A search for a solution was made for several fixed values of  $q$  using as adjustable parameters the inclination of the systems  $i$ , the mean temperature of the secondaries  $T_2$ , the surface potentials  $\Omega_1 = \Omega_2$ , and the monochromatic luminosities of the primaries  $L_1$ .

The behavior of the sum of squares of residuals,  $\Sigma(res)^2$ , was used to estimate a best value.

Then the value of  $q$  corresponding to the minimum of  $\Sigma(res)^2$  was included in the list of the adjustable parameters and a more detailed analysis was performed.

As shown in Figure 3, the light curves display an evident inverse O’Connell effect (O’Connell 1951) that should not be ignored. The maximum at phase 0.25 (Max I) is clearly fainter than that at phase 0.75 (Max II). In Table 4 we can see that the value of this asymmetry decreases from short to long wavelength; this is an indication that the spot is wavelength dependent and hotter than the surface temperature.

We therefore placed a spot at a fixed latitude  $90^\circ$  (i.e. on the equator) on the surface of the more massive component. The other spot parameters: longitude  $\phi$ , angular radius  $\gamma$  and the temperature factor  $T_s/T_*$ , were treated as free parameters and modified along with the adjustable system parameters.

The final derived photometric solution is listed in Table 5. The temperature factor of the spot suggests to us that it is possibly due to the impact from the mass transfer between the components (Lee et al. 2006).

The final synthetic light curves calculated with the whole set of parameters of Table 5 are shown in Figure 3 as continuous lines.

The observed and the theoretical light curves are in good agreement. A graphic representations and the Roche geometry of the systems is shown in Figure 4.

In this paper we use the output errors from the DC program keeping in mind that the errors here indicated are the formal errors and are unrealistically small; for a discussion see Barani et al. (2017).

The results of our analysis indicate that J213033 is an A-subtype DLMLR system with a low orbital inclination of  $62^\circ$ , while J212454 is a W-subtype shallow-contact binary with a degree of contact lower than 20% (Liu et al. 2016) and a large orbital inclination of  $88^\circ$ . This result implies that it is a totally eclipsing binary system and the photometric parameters here obtained are quite reliable (Terrell & Wilson 2005).

#### 4. EVOLUTIONARY STATE OF THE SYSTEMS

In the absence of spectroscopic elements the absolute parameters cannot be determined directly. However, preliminary absolute elements were derived for each star of both systems using the values from Table 5.

As the two systems belong to different subtypes of the W UMa contact binaries, in the estimation of the absolute parameters we used two different relationships. For J213033 we estimated the global parameters using the empirical relationship “period - total mass” by Yang & Qian (2015) for low mass-ratio binaries through the following formulae.

$$M_{total} = 0.5747(\pm 0.0160) + 2.3734(\pm 0.0331) \times P, \quad (4)$$

$$\log_{10}(R_1/R_\odot) = 0.0751(\pm 0.0014) + 0.9513(\pm 0.0086) \times \log_{10}(M_1/M_\odot), \quad (5)$$

$$\log_{10}(R_2/R_\odot) = 0.2826(\pm 0.0035) + 0.6177(\pm 0.0050) \times \log_{10}(M_2/M_\odot). \quad (6)$$

The derived mean densities of the components,  $\rho_1$  and  $\rho_2$  are estimated according to Mochnacki (1981), the luminosities are calculated using the following formula by Milano & Russo (1983).

$$L_{1,2} = R_{1,2}^2 \times (T_{1,2}/T_\odot)^4 \text{ with } T_\odot = 5780K. \quad (7)$$

While for J212454 we used the “period-semi-major axis” ( $P, a$ ) relation by Dimitrov & Kjurkchieva (2015).

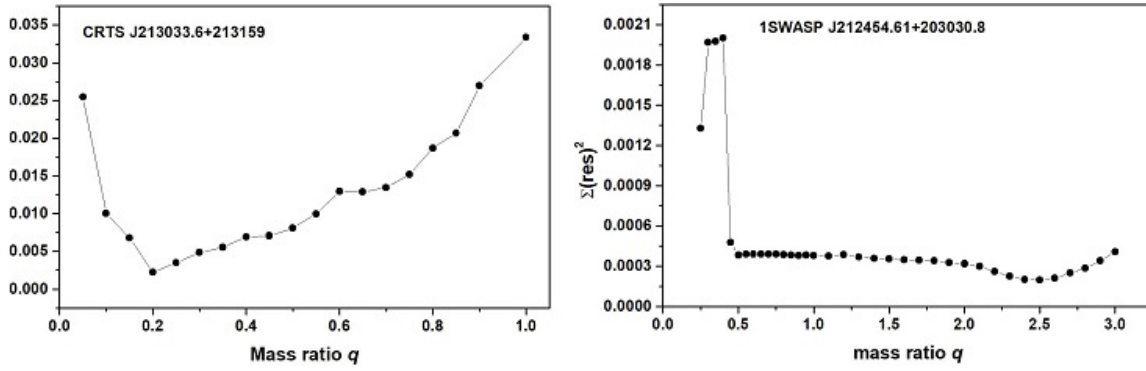


Fig. 2. The relation  $\Sigma(res)^2$  versus mass ratio  $q$  in Mode 3 for J213033 and for J212454.

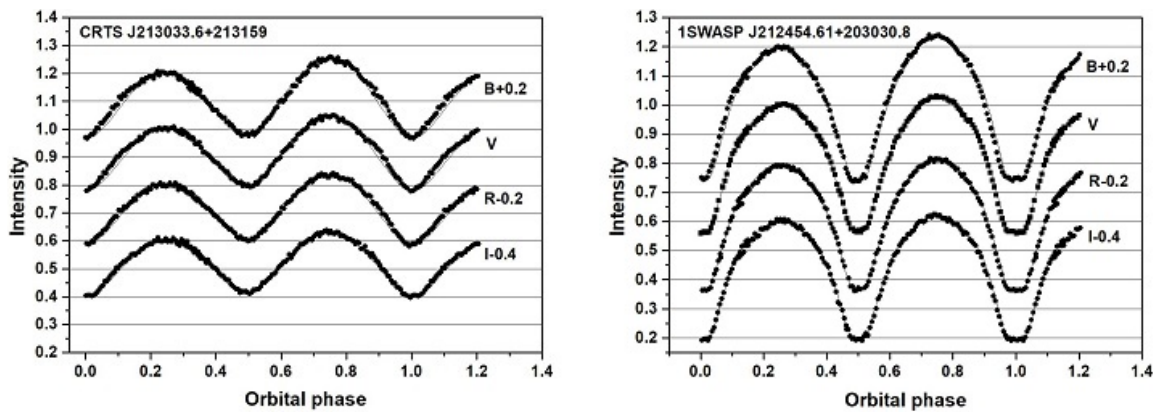


Fig. 3. CCD light curves of J2130033 and J212454. Points are the original observations and lines are the theoretical fits with the spot contribution.

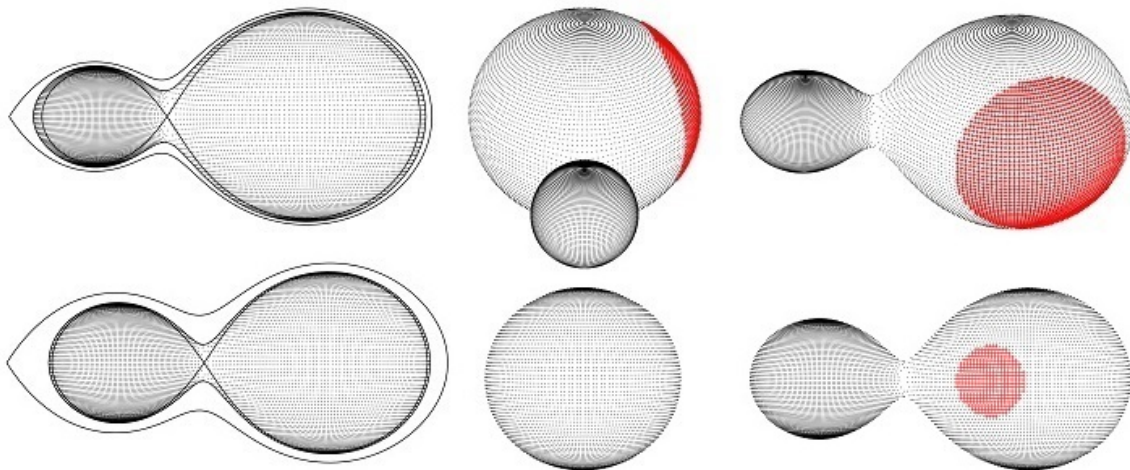


Fig. 4. Graphic representation of J313033 (up) and J212453 (down) according to our solution at quadrature (right) and at primary minimum (center). Left: the configuration of the components of the systems in the orbital plane is shown. The color figure can be viewed online.

TABLE 5  
LIGHT CURVE SOLUTIONS FOR J213033  
AND J212454<sup>1</sup>

Parameter	J213033	J212454
$i$ ( $^\circ$ )	$62.022 \pm 0.272$	$88.588 \pm 0.220$
$T_1$ (K)	5200*	5190*
$T_2$ (K)	$5200 \pm 25$	$5080 \pm 12$
$\Omega_1 = \Omega_2$	$2.136 \pm 0.002$	$5.824 \pm 0.002$
$q = m_2/m_1$	$0.186 \pm 0.001$	$2.486 \pm 0.003$
$A_1 = A_2$	0.5*	0.5*
$g_1 = g_2$	0.32*	0.32*
$L_{1B}$	$0.762 \pm 0.006$	$0.321 \pm 0.002$
$L_{1V}$	$0.769 \pm 0.005$	$0.317 \pm 0.001$
$L_{1R}$	$0.769 \pm 0.004$	$0.313 \pm 0.001$
$L_{1I}$	$0.773 \pm 0.004$	$0.311 \pm 0.001$
$L_{2B}$	$0.189 \pm 0.004$	$0.629 \pm 0.003$
$L_{2V}$	$0.188 \pm 0.004$	$0.636 \pm 0.003$
$L_{2R}$	$0.187 \pm 0.003$	$0.641 \pm 0.003$
$L_{2I}$	$0.187 \pm 0.003$	$0.656 \pm 0.002$
$f$	$0.517 \pm 0.006$	$0.168 \pm 0.007$
$X_{1B} = X_{2B}$	0.789*	0.794*
$X_{1V} = X_{2V}$	0.456*	0.461*
$X_{1Rc} = X_{2Rc}$	0.268*	0.271*
$X_{1Ic} = X_{2Ic}$	0.149*	0.151*
$L_3$	0	0
$r_1$ (pole)	$0.507 \pm 0.001$	$0.291 \pm 0.001$
$r_1$ (side)	$0.559 \pm 0.001$	$0.305 \pm 0.001$
$r_1$ (back)	$0.586 \pm 0.001$	$0.343 \pm 0.002$
$r_2$ (pole)	$0.246 \pm 0.002$	$0.440 \pm 0.001$
$r_2$ (side)	$0.258 \pm 0.002$	$0.472 \pm 0.001$
$r_2$ (back)	$0.311 \pm 0.006$	$0.501 \pm 0.001$
lat spot( $^\circ$ )	90*	90*
long spot( $^\circ$ )	$110.3 \pm 3.6$	$70.3 \pm 2.2$
radius( $^\circ$ )	$50.1 \pm 2.9$	$23.4 \pm 2.2$
Temp fac.Spot	$1.025 \pm 0.006$	$1.11 \pm 0.06$
Star	secondary	primary
Sum (res) <sup>2</sup>	0.0020	0.00019

<sup>1</sup>Assumed parameters are marked with \*.

Knowing the period of J212454 of  $0^d.2278293$ ,

$$a = -1.154 + 14.633 \times P - 10.319 P^2, \quad (8)$$

where  $a$  is in solar radii and  $P$  in days.

TABLE 6  
PRELIMINARY ABSOLUTE ELEMENTS FOR  
THE SYSTEMS

J213033	Primary	Secondary
Mass( $M_\odot$ )	$0.995 \pm 0.001$	$0.185 \pm 0.001$
Radius( $R_\odot$ )	$1.183 \pm 0.001$	$0.676 \pm 0.002$
Luminosity( $L_\odot$ )	$0.917 \pm 0.002$	$0.3 \pm 0.002$
$\log g$ (cgs)	4.29	4.04
$\rho$ (gr/cm <sup>3</sup> )	1.47	2.27
$a$ ( $R_\odot$ )	$1.841 \pm 0.003$	
J212454	Primary	Secondary
Mass( $M_\odot$ )	$0.818 \pm 0.010$	$0.329 \pm 0.003$
Radius( $R_\odot$ )	$0.775 \pm 0.005$	$0.515 \pm 0.005$
Luminosity( $L_\odot$ )	$0.358 \pm 0.003$	$0.172 \pm 0.003$
$\log g$ (cgs)	4.57	4.53
$\rho$ (gr/cm <sup>3</sup> )	2.484	3.405
$a$ ( $R_\odot$ )	$1.644 \pm 0.002$	

The  $(P, a)$  relation (equation 8) corresponds to the following relation “period-mass” for short-period binaries

$$M = (0.0134/P^2) \times a^3, \quad (9)$$

where  $M$  is the total mass of the binary.

The full set of preliminary absolute parameters is shown in Table 6. These values can be used in statistical diagrams to understand the evolutionary state of the components.

Using the list of 46 DLMLR binaries published by Yang & Qian (2015) and the seven new systems found in the literature (Table 7), we show the position of J213033 in the evolutionary diagram of Figure 5. Both components of our system follow the general pattern of the DLMLR shown in the example: the primaries are evolved or slightly evolved from the ZAMS, and the secondary stars are not evolved.

In Figure 6 we plot the components of J212454 together with other W- and A-type W UMa systems collected by Yankut & Eggleton (2005) and Li et al. (2008) on the logarithmic mass-luminosity ( $M-L$ ) relationship, along with the ZAMS and TAMS computed by Girardi et al. (2000).

It is clear from this figure that both components of J212454 are in good agreement with the well known W-type W UMa systems on the  $\log M - \log L$  plane.

TABLE 7

PHOTOMETRIC AND ESTIMATED ABSOLUTE ELEMENTS OF SEVEN NEW DLMR SYSTEMS

System	Period (days)	$T_1$ (K)	$T_2$ (K)	$q$	$f$ (%)	$M_1$ ( $M_\odot$ )	$M_2$ ( $M_\odot$ )	$R_1$ ( $R_\odot$ )	$R_2$ ( $R_\odot$ )	$L_1$ ( $L_\odot$ )	$L_2$ ( $L_\odot$ )	Ref.
ASAS 050334-2521.9	0.41407	6347	5925	0.133	53	1.260	0.168	1.540	0.600	3.450	0.400	1
ASAS 063546-1928.6	0.475515	6229	6072	0.173	58	1.190	0.206	1.630	0.700	3.600	0.600	1
TYC 1174-344-1	0.3887	6500	6357	0.187	51.8	1.381	0.258	1.449	0.714	3.310	0.736	2
TYC 2058-753-1	0.3532	5370	5394	0.103	64	1.030	0.110	1.270	0.460	1.200	0.160	3
TY Pup	0.8192	6900	6915	0.184	84.3	1.650	0.303	2.636	1.373	14.112	3.862	4
V53-M4	0.3084	7415	6611	0.078	69.1	1.470	0.115	1.383	0.481	7.306	0.465	5
V658 Lyr	0.330257	5752	5628	0.179	50.1	1.180	0.210	1.240	0.600	1.520	0.330	6

Ref. (1) Gezer & Bozkurt (2016), (2) Gürol et al. (2011), (3) Alton (2018), (4) Sarotsakulchai et al. (2018), (5) Li et al. (2017), (6) Martignoni et al. (2018).

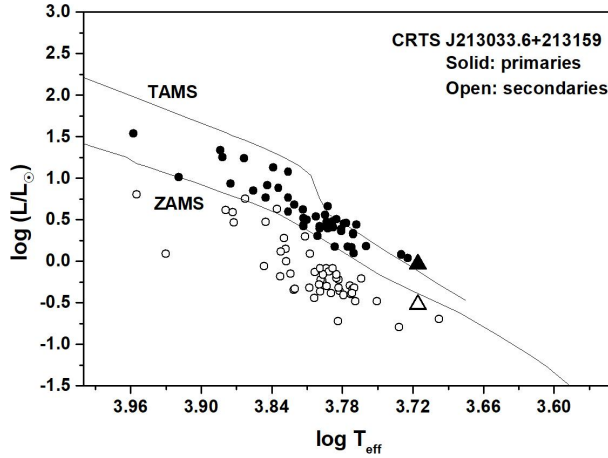


Fig. 5. Position of the components of J213033 in the  $\log T - \log L$  diagram. Zero Age Main Sequence (ZAMS) and Terminal Age Main Sequence (TAMS) are taken from Girardi et al. (2000) for solar chemical composition.

The location of the primary component of the system is near the ZAMS line; that means that is not yet evolved. On the other hand, the secondary component deviates significantly from the ZAMS.

With the absolute elements of Table 6 we can infer the dynamical evolution of the binary orbit of the systems using the orbital angular momentum  $J_0$  (Eker et al. 2006). In their paper, Eker et al. investigated 119 chromospherically active binaries (CAB) and 102 W UMa stars by means of the orbital angular momentum (OAM,  $J_0$ ) and systemic mass ( $M$ ): they found in the  $\log J_0 - \log M$  diagram a curved borderline separating the detached and the contact systems. The physical significance of this line is that it marks the maximum OAM for a contact system

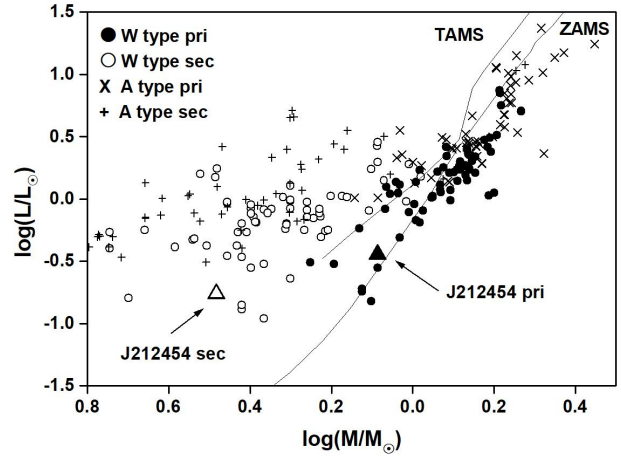


Fig. 6. Location of the components of J212454 on the  $\log M - \log L$  diagram.

to survive. If the OAM of a contact system is more than  $J_{lim}$  the contact configuration breaks.

The values of  $\log J_0 = 51.14$  obtained for J213033 and  $\log J_0 = 51.39$  for J212454 place our systems in the region of contact stars in the  $\log J_0 - \log M$  diagram shown in Figure 7.

## 5. DISCUSSION AND CONCLUSION

CRTS J213033.6+213159 is found to be an A-subtype contact binary with a low mass ratio of  $q = 0.186 \pm 0.001$  and showing a high fill-out parameter of  $f = 51.7 \pm 0.6\%$ . With these characteristics the system belongs to the class of the deep low mass ratio (DLMR) eclipsing binaries as proposed by Qian et al. (2005).



TABLE 8  
PARAMETERS OF THE PROGENITORS OF J212454

Mass parameter	Value
Current mass of the secondary $M_2$	$0.818M_{\odot} \pm 0.010$
Initial mass of the secondary $M_{2i}$	$0.426M_{\odot} \pm 0.090$
Current mass of the primary $M_1$	$0.329M_{\odot} \pm 0.003$
Initial mass of the primary $M_{1i}$	$1.223M_{\odot} \pm 0.090$
Orbital period of the first overflow PFOF	$0^d.85409 \pm 0.049$
Semi-major axis at the first overflow	$4.552R_{\odot} \pm 0.070$
J current angular momentum	$1.95^{51} \text{ cgs} \pm 0.050$
$J_{fof}$ angular momentum at the first overflow	$5.59^{51} \text{ cgs} \pm 0.049$
Mlost	$0.594M_{\odot} \pm 0.010$

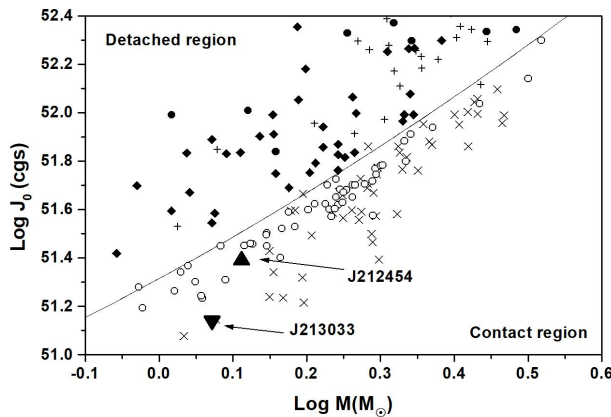


Fig. 7. The position of our systems in the  $\log J_0 - \log M$  diagram. Symbols are described in Figure 1 of the original paper of Eker et al. (2006).

1SWSP J212454.61+203030.8 is found to be an W-subtype with a mass ratio of  $q = 2.486 \pm 0.002$  ( $q_{inv} = 0.402$ ) and a shallow fill-out parameter of  $f = 16.8 \pm 0.7\%$ . Note that most of the W-subtype contact systems have shallow contact characteristics. The high orbital inclination  $i = 88.6^\circ$  tell us that the system is totally eclipsed and that the photometric parameters here obtained are reliable.

Yildiz & Dogan (2013) developed a method for the computation of initial masses of contact binaries based on the assumption that the mass transfer starts near or after the TAMS phase of the initially massive component, which is the currently less massive component.

They discovered that binary systems with an initial secondary mass higher than  $1.8 \pm 0.1M_{\odot}$  become A subtype, while systems with initial masses lower than this become W subtype.

We can apply the method to J212454, to be able to calculate the absolute parameters of the detached system, progenitor of the contact system, as shown in Table 8.

We found that the initial mass of the secondary component would be  $0.426M_{\odot}$ , that means, J212454 has evolved to a W subtype, as predicted.

The results show that the angular momentum has decreased from  $5.51 \times 10^{51}$  cgs at the first overflow (FOF) to  $1.95 \times 10^{51}$  cgs at the present time, concurrently with a mass lost by the system of  $0.594M_{\odot}$ . Consequently, the orbital period and the semi-major axis have decreased from 0.7673105 days and  $4.555R_{\odot}$  to 0.22278293 days and  $1.841R_{\odot}$ , respectively.

Initially, the binary J212454, in the detached phase, consisted of two main sequence stars. The more massive component (the progenitor of the secondary component) evolved to the TAMS. In combination with the AML, the Roche surface was filled by the evolved secondary component, allowing the mass transfer to begin. Since the FOF until the present time, the orbit has decreased by the AML and mass loss. The angular momentum has been lost to 74.6% of  $J_{fof}$  from the stage at the FOF to the present time, producing a smaller orbit.

Two possible mechanisms were examined and we concluded that the continuous period decrease of J212454 is maybe not caused by a thermal mass transfer from the primary to the secondary component, but rather by angular momentum loss due to a magnetic stellar wind.

According to the parameters obtained for the system, we have drawn the configuration of the components using the Binary Maker 3.0 software (Bradstreet & Steelman 2002), which is shown in Figure 3.



For both the systems the small difference in temperature between the components suggest to us that they are in good thermal contact in spite of their different masses and radii.

The light curves of J213033 and J212454 exhibit the inverse O'Connell effect (O'Connell 1951) with the maximum at phase 0.25 (Max I) slightly fainter than that at phase 0.75 (Max II). For this reason a hot spot was placed on the surface of the more massive component.

While for J212454 the hot spot may indicate a probable impact from mass transfer between the components, for J213033 according to Sarotsakulchai et al. (2019), how large a hot spot ( $50^\circ$ ) should appear on the contact binary system is still unknown.

Both systems belong to spectral type K and are short period ( $< 0.3$  days) contact binaries.

The systems of spectral K-type are important to explain the period cutoff phenomenon, as argued by Liu et al. (2014), and to test the thermal relaxation oscillation theory (TRO theory Lucy 1976, Flannery 1976, Robertson & Eggleton 1977, Yankut & Eggleton 2005, Li et al. 2008).

Presumably, J213033 should be in an extreme phase of contact of the TRO cycle while the opposite should hold for J212454, due to its low fill-out value. However, the available observations are insufficient to reveal any period changes that could explain the behaviour of the mass ratio of the binary system.

Absolute parameters were estimated for the components. Based on these, we discussed the evolutionary status of the systems and concluded that the components of J213033 follow the general pattern of other DLMR, with the primary component evolved or slightly evolved from ZAMS and the secondary situated on the ZAMS, as an unevolved star.

The primary component of J212454 is an unevolved ZAMS star, while the secondary component deviates significantly from ZAMS.

Following the study of Eker et al. (2006) our systems, as expected, are located in the contact region of the  $\log J_0 - \log M$  diagram.

This research has made use of the International Variable Star Index (VSX) database, operated at AAVSO, Cambridge, Massachusetts, USA; of the VizieR catalogue access tool, CDS, Strasbourg, France. The original description of the VizieR service was published in A&AS 143, 23.

We acknowledge our anonymous referee for comments that helped to improve this work.

## REFERENCES

- Alton, K. B. 2018, JAVSO, 46, 1  
 Barani, C., Martignoni, M., & Acerbi, F. 2017, *NewA*, 50, 73  
 Binnendijk, L. 1965, *VeBam*, 27, 36  
 Bradstreet, D. H. & Steelman, D. P. 2002, *AAS*, 201, 7502  
 Butters, O. W., West, R. G., Anderson, D. R., et al. 2010. *A&A* 520, 10  
 Csizmadia, Sz. & Klagyvivik, P. 2004, *A&A*, 426, 1001  
 Dimitrov, D. P. & Kjurkchieva, D. P. 2015, *MNRAS*, 448, 2890  
 Drake, A. J., Graham, M. J., Djorgovski, S. G., et al. 2014, *ApJS*, 213, 9  
 Eker, Z., Demircan, O., Bilir, S., & Karataş, Y. 2006, *MNRAS*, 373, 1483  
 Flannery, B. P. 1976, *ApJ*, 205, 217  
 Gezer, İ. & Bozkurt, Z. 2016, *NewA*, 44, 40  
 Girardi, L., Bressan, A., Bertelli, G., & Chiosi, C. 2000, *A&AS*, 141, 371  
 Guinan, E. F. & Bradstreet, D. H. 1988, in *Kinematic Clues to the Origin and Evolution of Low Mass Contact Binaries*, eds. A. K. Dupree and M. T. V. T. Lago, (Springer, Dordrecht), 345  
 Gürol, B., Derman, E., Saguner, T., et al. 2011, *NewA*, 16, 242  
 Henden, A. A., Welch, D. L., Terrell, D., & Levine, S. E. 2009, *AAS*, 41, 669  
 Kwee, K. K. 1958, *BAN*, 14, 131  
 Lee, J. W., Lee, Ch., Kim, Ch., & Kang, Y. W. 2006, *JKAS*, 39, 41  
 Li, K., Hu, S., Chen, X., & Guo, D. 2017, *PASJ*, 69, 79  
 Li, L., Zhang, F., Han, Z., Jiang, D., & Jiang, T. 2008, *MNRAS*, 387, 97  
 Liao, W.-P., Qian, S.-B., Soonthornthum, B., et al. 2017, *PASP*, 129, 124204  
 Liu, N.-P., Qian, S.-B., Soonthornthum, B., et al. 2014, *AJ*, 147, 41  
 Liu, L., Qian, S. B., He, J. J., et al. 2016, *NewA*, 43, 1  
 Lohr, M. E., Norton, A. J., Kolb, U. C., et al. 2013, *A&A*, 549, A86  
 Lucy, L. B. 1967, *ZA*, 65, 89  
 \_\_\_\_\_. 1976, *ApJ*, 205, 208  
 Lucy, L. B. & Wilson, R. E. 1979, *ApJ*, 231, 502  
 Martignoni, M., Barani, C., & Acerbi, F. 2018, *NewA*, 62, 121  
 Milano L. & Russo G. 1983, *MNRAS*, 203, 235  
 Mocknacki, S. W. 1981, *ApJ*, 245, 650  
 O'Connell, D. J. K. 1951, *PRCO*, 2, 85  
 Norton, A. J., Payne, S. G., Evans, T., et al. 2011, *A&A*, 528, 90  
 Paczyński, B. 1971, *ARA&A*, 9, 183  
 Qian, S.-B., Yang, Y.-G., Soonthornthum, B., et al. 2005, *AJ*, 130, 224  
 Robertson, J. A. & Eggleton, P. P. 1077, *MNRAS*, 179, 359  
 Ruciński, S. M. 1973, *AcA*, 23, 79

- Sarotsakulchai, T., Qian, S.-B., Soonthornthum, B., et al. 2018, *AJ*, 156, 199
- Sarotsakulchai, T., Qian, S.-B., Soonthornthum, B., et al. 2019, *PASJ*, 71, 81
- Stępień, K. 2011, *AcA*, 61, 139
- Terrell, D. & Wilson, R. E. 2005, *Ap&SS*, 296, 221
- Tylenda, R., Hajduk, M., Kamiński, T., et al. 2011, *A&A*, 528, 114
- van Hamme, W. 1993, *AJ*, 106, 2096
- Wang, J.-M. 1994, *ApJ*, 434, 277
- Webbink, R. F. 1976, *ApJ*, 209, 829
- Wilson, R. E. & Devinney, E. J. 1971, *ApJ*, 166, 605
- Wilson, R. E. 1990, *ApJ*, 356, 613
- Wilson, R. E. & van Hamme, W. 2015, Computing binary stars observables, ([ftp.astro.ufl.edu](ftp://ftp.astro.ufl.edu)), directory [pub/wilson/lcdc2015](http://pub/wilson/lcdc2015)
- Worthey, G. & Lee, H. C. 2011, *ApJS*, 193, 1
- Yang, Y.-G. & Qian, S.-B. 2015, *AJ*, 150, 69
- Yankut, K. & Eggleton, P. P. 2005, *ApJ*, 629, 1055
- Yildiz, M. & Doğan, T. 2013, *MNRAS*, 430, 2029
- Zhu, L.-Y., Zhao, E.-G., & Zhou, X. 2016, *RAA*, 16, 68

- F. Acerbi: Via Zoncada 51, Codogno, LO, 26845, Italy ([acerbifr@tin.it](mailto:acerbifr@tin.it)).
- C. Barani: Via Molinetto 35, Triulza di Codogno, LO, 26845, Italy ([cvbarani@alice.it](mailto:cvbarani@alice.it)).
- M. Martignoni: Via Don G. Minzoni 26/D, Magnago, MI, 20020, Italy ([massimiliano.martignoni@alice.it](mailto:massimiliano.martignoni@alice.it))
- R. Michel: Universidad Nacional Autónoma de México. Observatorio Astronómico Nacional. Apartado Postal 877, C.P. 22800, Ensenada, B.C., México ([rmm@astro.unam.mx](mailto:rmm@astro.unam.mx)).